Dynamic constitutive equation of GFRP obtained by Lagrange experiment

SHANG Jialan[1], BAI Yilong[1], XU Suzhen[2] & CAI Xiaoye[1]

1. Institute of Mechanics, Chinese Academy of Sciences, Beijing 100080, China;
2. Beijing Institute of Special Electronic and Mechanical Devices, Beijing 100076, China

Abstract The note presents a method of constructing dynamic constitutive equations of material by means of Lagrange experiment and analysis. Tests were carried out by a light gas gun and the stress history profiles were recorded on multiple Lagrange positions. The dynamic constitutive equations were deduced from the regression of a series of data which was obtained by Lagrange analysis based upon recorded multiple stress histories. Here constitutive equations of glass fibre reinforced phenolic resin composite(GFRP) in uniaxil strain state under dynamic loading are given. The proposed equations of the material agree well with experimental results.

Keywords: impact loading, dynamic constitutive equation, Lagrange analysis.

Dynamic constitutive relationship is a fundamental characteristic of mechanical behaviour of meterials under impulsive loading. The relation between the strain rate at 10^3-10^5 s and the stress in 10^2-10^3 MPa is essential for the design and the structure study under impact. For traditional materials, three kinds of practical constitutive theories based on experiment have been widely used. They are over-stress, visco-plastic and elastic-viscoplastic model theories[1,2]. In recent years, a number of new materials, such as reinforced composites, have been increasingly adopted in designing structures under impact.

For these materials, however, it is difficult to assume a proper constitutive model. So a set of digital and graphical representation for the constitutive relation was obtained by Lagrange experiment. A technique, developed by the Laboratory for Nonlinear Mechanics of the Institute of Mechanics, Chinese Academy of Sciences, was employed to apply Lagrange analysis to the data obtained from plate impact and multiple stress measurement[3,4]. Based on this, the physical characteristics of material, such as the hysteresis, strain rate, strain and strain rate history effect were discussed. In addition, a modulus function, a rate-type quantity expressed in terms of strain and strain rate, was found. Then a set of complete and usable constitutive equations was established.

1 Experiment and analysis of measured records

The test material is glass fiber reinforced phenolic resin composite (GFRP) with density ρ_0 =1 640 kg/m^3 and wave speed in uniaxial strain state 3 140 m/s. The static tensile strength perpendicular to the fibre plies is 5.7—5.8 MPa and along the plies 20.4 MPa. There are 5 plies in every 1-mm thickness.

Symmetrical plate impact experiments were carried out on a 101-mm bore light gas gun shown in fig. 1(a). The stress history was monitored by carbon piezoresistance gages embedded in different positions within the specimen as shown in fig. 1(b). The impact velocity was in the range of 170—530 m/s. A typical set of stress profiles is illustrated in fig. 1(c), where v is the impact velocity.

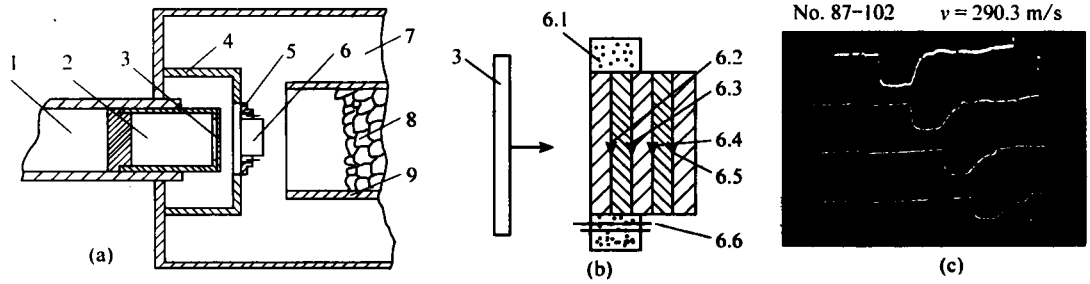

Fig. 1. Scheme of planar plate impact experiment (a), arrangement of gages embedded in target (b) and a photo of stress profiles (c). 1, Barrel; 2, sabot; 3, flyer; 4, target holder; 5, target ring; 6, target specimen; 7, sealed chamber; 8, buffer; 9, catcher. 6.1, Epoxy; 6.2-6.5, stress gage 1 ($k = 0$), 2 ($k = 2$), 3 ($k = 4$), 4 ($k = 6$), respectively; 6.6, pins.

The data were then processed by the Lagrange analysis method (LAM), which was first proposed by Fowles[5], Williams and Cowperthaeite[7] and later improved by Grady[8] and Seaman[6]. The constitutive equations can be obtained by this method directly from stress wave profiles without any model assumption to the material. The LAM used was based on the measured multiple stress profiles of a single test, and the internal variables of material were obtained from continuity and momentum conservation. This is a preferable way of solving an inverse problem in mechanics due to its reflection of the physical characteristics of material[9].

A graphical representation of the relationship between stress, stress gradient and strain vs. strain rate is shown in fig. 2(a). The stress-strain relations of the six tests under various stress loading levels are given in fig. 2(b). It is shown that a higher loading level corresponds to a higher strain rate.

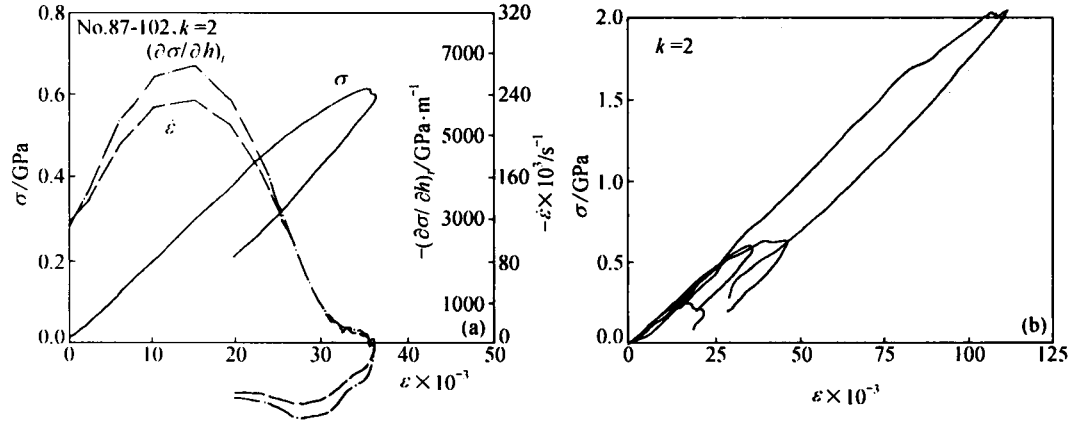

Fig. 2. Analytical results. (a) Relationship among the stress σ, strain rate $\dot{\varepsilon}$ and stress gradient $\left.\frac{\partial\sigma}{\partial h}\right|_t$ vs. volume strain. (b) stress-strain relation of the six experiments at different loading levels.

2 Character of the dynamic constitutive data of GFRP

The stress-strain σ-ε curves in fig. 2 illustrate the undergone process in a GFRP element during the test. In fig. 2, the σ-ε curves are convex during loading while concave during unloading. When ε reaches 30×10^3 $\mu\varepsilon$, the stress-strain curves fall down towards the ε-coordinate, but the strain-strain rate curves keep close to the ε-coordinate. The material comes to a crop state because the strain is still increasing. The σ-ε curves show distinctive hysteresis, of which the tensity is controlled by the

magnitude of the strain rate. Moreover, fig. 2(a) also shows that while the strain is increasing, the strain rate, stress and strain reach their maxima one after the other. When the strain rate changes from 40×10^3 to 385×10^3 s^{-1}, the maximal variations in the ratio of these maxima $\dot{\varepsilon}_m/\sigma_m$ and $\dot{\varepsilon}_m/\varepsilon_m$ are 10% and 20%, respectively. This demonstrates that the peak stress and peak strain vary at the same order as the strain rate, they thus indicate that σ_m and $\dot{\varepsilon}_m$ are related to the magnitude of the strain rate.

Considering the rate type quantity $R=\left.\frac{d\sigma}{d\varepsilon}\right|_h$ as the derivative of the σ - ε curve, it is shown from fig. 3 that stress waves through an element can be illustrated by the R-ε curve. Upon loading, ε increases from zero and R remains high. R then decreases gradually with the increasing ε. It becomes zero when the stress reaches its maximum. Afterwards, R drops faster and faster till $R=-\infty$ when the strain reaches its maximum. Finally, during unloading both stress and strain decrease, and R falls rapidly from a very high value (or $+\infty$) to a limit, which is higher than its initial loading value.

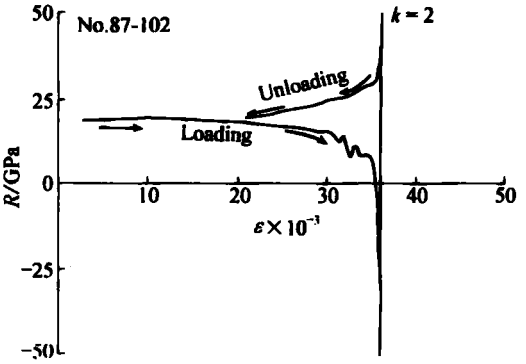

Fig. 3. Relation between the modulus function R and the volume strain ε.

In short, the dynamic constitutive relation of GFRP has the following features: (i) The stress, strain and strain rate under impact all change with time. (ii) The transient stress is related not only with the transient strain and transient strain rate but also with histories of the strain and strain rate. Because of this obvious non-equilibrium effect, there seems to be no simple algebraic equations among σ, ε, and $\dot{\varepsilon}$. (iii) Observing the relationship among σ, ε and $\dot{\varepsilon}$ of materials upon impact, a probable way of solving this problem is to find out the relationship among rate-type quantities.

3 Modulus function $R(\varepsilon, \dot{\varepsilon})$

One of these rate-type quantities is modulus function R

$$R(\varepsilon,\dot{\varepsilon})=\left.\frac{d\sigma}{d\varepsilon}\right|_h=\frac{\dot{\sigma}}{\dot{\varepsilon}}, \tag{1}$$

Where $R(\varepsilon,\dot{\varepsilon})$ is the gradient of σ-ε curve and the ratio of the stress rate to the strain rate. It identifies rigidity of a kind of material. Fig. 3 plots the typical R-ε relation in an element subjected to stress waves. In the range of large strain, R decreases rapidly, indicating that the material loses its rigidity because of its decreasing modulus.

The test results of loading up to various peak stress provide a quite unique R-ε relation. Fig. 4 shows that for various ε there is a roughly same tendency in the $\dot{\varepsilon}$ relation. Fig. 4 represents the loading (a) and the unloading process (b). In fig. 4(a), R approaches a saturation value R_0 when ε is large. When ε decreases, R decreases more and more rapidly and approaches a large negative value when ε closes to zero. The difference between the R-ε curves at different ε shows a similar tendency in $\dot{\varepsilon}$ as shown in fig. 4(b). It can be seen that in process of strain loading and unloading, the given $R(\varepsilon,\dot{\varepsilon})$ can be grouped into two families of hyperbolic curves with a little difference for different ε. Their representative forms can be regressed as follows:

$$R=R_0\left[1-A(\varepsilon)\left(\frac{\dot{\varepsilon}}{\dot{\varepsilon}^*}\right)^{-m}\right],\quad d\varepsilon>0, \tag{2}$$

$$R = R_{u0}\left[1 + R_{u1}\varepsilon + B(\varepsilon)\left(-\frac{\dot{\varepsilon}}{\dot{\varepsilon}^*}\right)^{-n}\right], \quad d\varepsilon < 0, \tag{3}$$

where $\dot{\varepsilon}^* = 10^3\ s^{-1}$. $R_0 = 22.5$ GPa, $R_{u0} = 13.5$ GPa, $R_{u1} = 12.1$, $m = 0.55$ and $n = 1.44$.

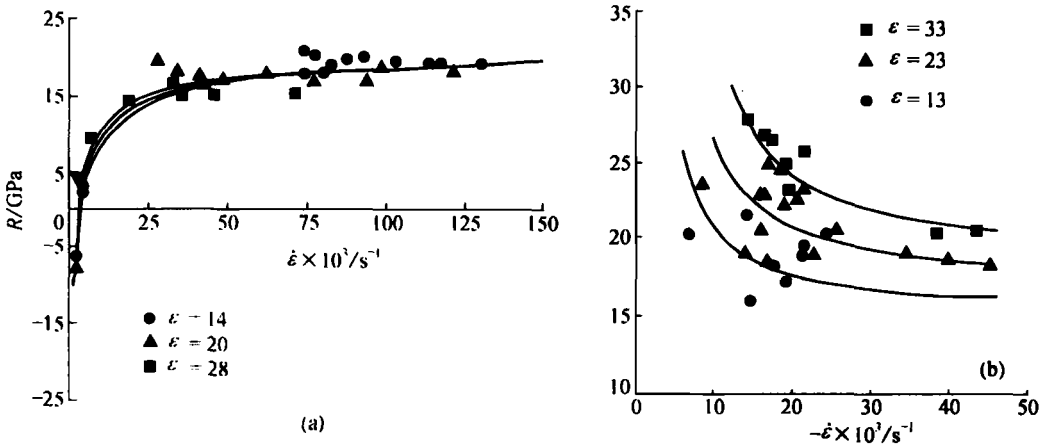

Fig. 4. When ε = const., relation of R with $\dot{\varepsilon}$. (a) $d\varepsilon>0$, (b) $d\varepsilon<0$.

$A(\varepsilon)$ and $B(\varepsilon)$ are functions of ε and can be fitted as the following two third power series,

$$A(\varepsilon) = \sum_{i=0}^{3} A_i \varepsilon_i\ , \tag{4}$$

$$B(\varepsilon) = \sum_{i=0}^{3} B_i \varepsilon_i\ , \tag{5}$$

where $A_0 = 0.991$, $A_1 = 0.902\times10^2$, $A_2 = -1.85\times10^3$, $A_3 = 7.69\times10^3$, $B_0 = -5.48$, $B_1 = 1.36\times10^3$, $B_2 = -1.16\times10^4$ and $B_3 = 3.48\times10^4$.

However, it should be noted that eqs. (2) and (3) are valid while the initial loading has a high strain rate 10^3—$10^4\ s^{-1}$. In the tested material, the strong wave was propagating which was caused by high velocity impact. In fig. 4 the region of $\begin{Bmatrix} R<0 \\ \dot{\varepsilon}\to 0 \end{Bmatrix}$ and $\begin{Bmatrix} \dot{\varepsilon}\to 0 \\ R\to 0 \end{Bmatrix}$ is corresponding to that of the stress decreasing initially from σ_m while strain is still increasing.

4 The dynamic constitutive equation of GFRP

Eqs. (2) and (3) describe the change of the modulus function when plane stress waves are under impact loading. From eq. (1) there is

$$\dot{\sigma} = R(\varepsilon, \dot{\varepsilon})\dot{\varepsilon}\ . \tag{6}$$

Then the differential form of dynamic constitutive equations of GFRP is

$$\dot{\sigma} = R_0\left[1 - A(\varepsilon)\left(\frac{\dot{\varepsilon}}{\dot{\varepsilon}^*}\right)^{-m}\right]\dot{\varepsilon}, \quad d\varepsilon > 0, \tag{7a}$$

$$\dot{\sigma} = R_0\left[\varepsilon - \int_0^{\varepsilon} A(\varepsilon)\left(\frac{\dot{\varepsilon}}{\varepsilon^*}\right)^{-m} d\varepsilon\right]\dot{\varepsilon}, \quad d\varepsilon < 0\ . \tag{7b}$$

At $t = 0$, $\sigma = 0$, $\varepsilon = 0$, the stress in the material is

$$\sigma = R_0\left[\varepsilon - \int_0^{\varepsilon} A(\varepsilon)\left(\frac{\dot{\varepsilon}}{\dot{\varepsilon}*}\right)^{-m} d\varepsilon\right], \quad d\varepsilon > 0, \tag{8a}$$

and

$$\sigma = \sigma|_{\varepsilon=\varepsilon_m} + R_{u0}\left[(\varepsilon-\varepsilon_m) + \frac{R_{u1}}{2}(\varepsilon^2-\varepsilon_m^2) + \int_{\varepsilon_m}^{\varepsilon} B(\varepsilon)\left(-\frac{\dot{\varepsilon}}{\dot{\varepsilon}*}\right)^{-n} d\varepsilon\right], \quad d\varepsilon < 0, \tag{8b}$$

where ε_m is the maximum of ε at $\dot{\varepsilon} = 0$. The first term in the right hand side of eq. 8(a) is a linear term. The second term indicates a combined result between softening from large deformation and hardening from high strain rate. R_0 is a saturation value of the modulus function under high strain rate loading. When ε approaches infinity, $R = R_0$, and the wave speed $c(\dot{\varepsilon}_\infty) = \sqrt{\frac{R_0}{\rho_0}} = 3.70$ km/s. Therefore, $c(\dot{\varepsilon}_\infty)$ is the limit speed of uniaxial strain plane waves under high strain rate loading. The highest wave speed in our measurement is 3.65 km/s.

The calculated result from eq. (8) is consistent with experimental σ-ε curves as shown in fig. 5(a). Denoting *ER* the relative error of the fitted result to experimental one, *ER* is generally less than 10% except in the initial loading stage, where the error is 20%. The average error during loading ($d\varepsilon>0$) is $ER<8.83\%$. The results of No. 87—102 and No. 87—113 are especially good, their average error $ER \leqslant \pm 2.1\%$ and the maximal average error $ER \leqslant \pm 4.3\%$. The error during unloading ($d\varepsilon<0$) is large due to the error accumulation. Nevertheless, the gradients of experimental and fitted curves are nearly the same. Fig. 5(b) shows another set of consistent results, where the test was not put into the regression for construction of the constitutive equations.

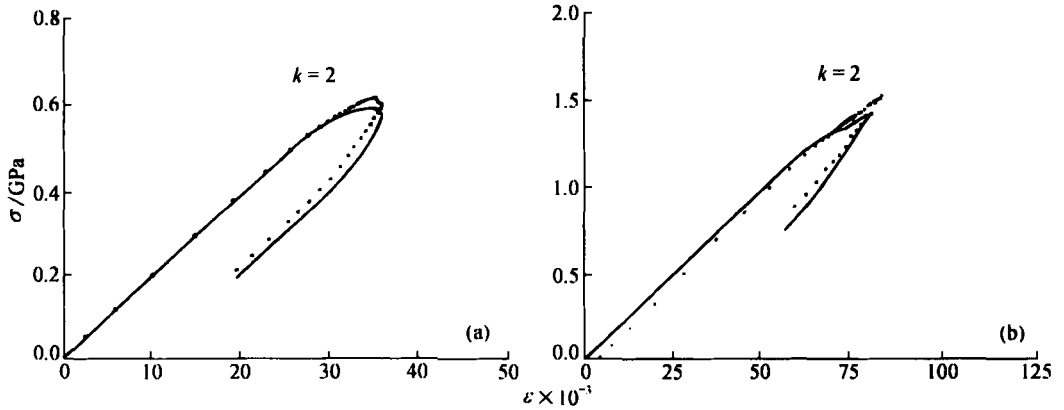

Fig. 5. σ-ε curves comparison of calculation value (solid line by eq. (8)) with the experimental value (dotted line). (a) Shot No. 87—102. (b) Shot No. 88—59, which was not ever used to regress the constitutive equation.

The validity of these obtained constitutive equations requires the following conditions: (i) the initial strain rate $\dot{\varepsilon} > 10^3\ s^{-1}$; (ii) the maximum stress $\sigma_m < 2.2$ GPa; (iii) the maximum strain $\sigma_m < 0.11$.

5 Summary

The constitutive equation of GFRP in uniaxial strain state under impact loading is presented in this note. It is obtained by means of regression to the numerical constitutive relation derived from the Lagrange analysis of multiple stress measurement. It fully reflects the physical characteristics of

material, such as the hysteresis, strain rate, strain history and strain rate history effect. The calculated results are in good agreement with experiment. As far as the authors know, this note is the first to report in such a way of constructing a set of complete and usable dynamic constitutive equations from the experiment for an unknown material.

Acknowledgements This work was supported by the Key Project of the National Natural Science Foundation of China (Grant No. 19132030).

References

1. Yang Guitong, Xiong Zhuhua, Plastic Dynamics (in Chinese), Beijing: Tsinghua University Press, 1984, 48.
2. Zhou Guangqian, Some discussion on elastic-viscoplastic theory with no yield surface, Explosion and Shock Waves (in Chinese), 1983, 3 (4): 25.
3. Zhou Shida, Shen Letian, Zhao Shuanglu, One stage light gas gun used in the dynamic property test of materials, Acta Armamentaii (in Chinese), 1985, 4: 49.
4. Shang Jialan, Bai Yilong, Shen Letian et al., Experimental studies of dynamical constitutive relation of glass fiber reinfoeced phenolic resin, Explosion and Shock Waves (in Chinese), 1990, 10(1): 1.
5. Fowles, G. R., Williams, R. F., Plane stress wave propagation in solid, JAP, 1970, 41(1): 360.
6. Cowperthwaite, M., Williams, R. F., Determination of constitutive relationships with multiple gauges in nondivergent waves, JAP, 1971, 4(1): 456.
7. Grady, D. E., Experimental analysis of spherical wave propagation, JGR, 1973, 78(8): 1299.
8. Seaman, L., Lagrangian analysis for multiple stress or velocity gages in attenuating waves, JAP, 1974, 45(10): 4303.
9. Tang Zhiping, Lagrangian analysis and its recent developments, Advances in Mechanics (in Chinese), 1993, 23(3): 348.

(Received June 13, 1999, accepted Feburary 2, 2000)